Mathematical Modelling and Numerical Simulation with Applications, 2024, 4(1), 110–132

https://dergipark.org.tr/en/pub/mmnsa

ISSN Online: 2791-8564 / Open Access

https://doi.org/10.53391/mmnsa.1428035

RESEARCH PAPER

Spectral collocation with generalized Laguerre operational matrix for numerical solutions of fractional electrical circuit models

İbrahim Avcı [1,*,‡]

[1]Department of Computer Engineering, Faculty of Engineering, Final International University, Kyrenia, Northern Cyprus, via Mersin 10, Türkiye

*Corresponding Author

‡ ibrahim.avci@final.edu.tr (İbrahim Avcı)

Abstract

In this paper, we introduce a pioneering numerical technique that combines generalized Laguerre polynomials with an operational matrix of fractional integration to address fractional models in electrical circuits. Specifically focusing on Resistor–Inductor (RL), Resistor–Capacitor (RC), Resonant (Inductor–Capacitor) (LC), and Resistor–Inductor–Capacitor (RLC) circuits within the framework of the Caputo derivative, our approach aims to enhance the accuracy of numerical solutions. We meticulously construct an operational matrix of fractional integration tailored to the generalized Laguerre basis vector, facilitating a transformation of the original fractional differential equations into a system of linear algebraic equations. By solving this system, we obtain a highly accurate approximate solution for the electrical circuit model under consideration. To validate the precision of our proposed method, we conduct a thorough comparative analysis, benchmarking our results against alternative numerical techniques reported in the literature and exact solutions where available. The numerical examples presented in our study substantiate the superior accuracy and reliability of our generalized Laguerre-enhanced operational matrix collocation method in effectively solving fractional electrical circuit models.

Keywords: Numerical analysis; electrical circuits; generalized Laguerre polynomials; fractional integrals; fractional derivatives

AMS 2020 Classification: 41A58; 26A33; 34A08

1 Introduction

In recent years, an escalating interest has emerged among researchers in harnessing the power of fractional calculus and Fractional Differential Equations (FDEs). Fractional calculus, a field rooted in the generalization of integration and differentiation to arbitrary orders, finds its origins in the

➤ **Received:** 29.01.2024 ➤ **Revised:** 30.03.2024 ➤ **Accepted:** 31.03.2024 ➤ **Published:** 31.03.2024

musings of G.W. Leibniz (1695) and L. Euler (1730). Despite its longstanding history, fractional calculus and the corresponding FDEs have only recently surged in attention and popularity, driven by their unparalleled ability to model complex phenomena. Various definitions of fractional derivatives, including Riemann–Liouville, Caputo, Grünwald–Letnikov, Weyl, Marchaud, Prabhakar, and others, populate the literature, underscoring the versatility of this mathematical tool. The Riemann-Liouville definition is among the earliest formulations in the field of fractional calculus. It emerged as a significant contribution to the theory's development, offering foundational insights into fractional derivatives and integrals. Caputo's definition, introduced later, has become widely used in engineering applications. Its effectiveness lies in its ability to accurately model systems commonly encountered in engineering problems. Particularly in scenarios where boundary conditions predominantly involve integer-order derivatives, Caputo's operator excels in providing precise representations of physical systems, especially those exhibiting intricate behaviors, thereby contributing to its popularity. Grünwald–Letnikov, Weyl, Marchaud, and Prabhakar provide alternative approaches, each tailored to specific analytical or computational demands. The flexibility offered by these definitions allows researchers to tailor their approach to the particular characteristics of the problem at hand, making fractional calculus a powerful tool in mathematical modeling. The history of this topic can be found in [1–5].

The interdisciplinary applications of fractional calculus span an impressive array of fields, expanding beyond bioengineering, biology, chaotic systems, control theory, economics, electrochemistry, finance, quantum mechanics, optics, oncology, physics, rheology, social sciences, viscoelasticity, and so on [6–16]. This expansive scope underscores the versatility and profound impact of fractional calculus in addressing intricate challenges across diverse scientific and engineering domains. As we delve into this multifaceted landscape, it becomes evident that the marriage of mathematical rigor with innovative numerical techniques is paving the way for groundbreaking advancements and novel solutions in scientific inquiry.

Fractional calculus emerges as a superior modeling framework, often outperforming traditional calculus, particularly in capturing memory effects crucial for describing long-term interactions [17, 18]. This distinctive feature enhances the accuracy of representing diverse dynamical and engineering models, becoming indispensable in scientific investigations. Confronted with the inherent difficulty of obtaining exact analytic solutions for nonlinear FDEs, researchers have developed an arsenal of numerical and approximate methods. In addition to spectral collocation [19], variational iteration [20], differential quadrature [21], adomian decomposition [22], fractional reduced differential transform [23], and wavelet methods [24–26], innovative techniques such as finite element method [27], and radial basis function methods [28] have been meticulously crafted to surmount these challenges. On the other hand, many numerical techniques for solving fractional models face limitations, including accuracy issues with complex dynamics and non-standard boundaries, computational inefficiency for large-scale simulations, and restricted applicability to specific equations or systems. Moreover, the lack of a clear geometric interpretation in fractional calculus complicates algorithm development, hindering intuitive understanding and implementation. Additionally, convergence and stability challenges arise, particularly with nonlinear or stiff equations. Addressing these limitations requires the development of novel techniques to improve accuracy, efficiency, and applicability across a wide range of fractional systems and boundary conditions. Electrical circuit models serve as fundamental tools in understanding and analyzing the behavior of electrical systems [29]. Among the widely studied circuit configurations are the RC (resistor-capacitor), RL (resistor-inductor), LC (inductor-capacitor), and RLC (resistor-inductor-capacitor) circuits. In the RC circuit, the combination of a resistor and a capacitor introduces time-dependent characteristics, influencing the circuit's response to input signals. The RL circuit, incorporating a resistor and an inductor, exhibits distinctive behaviors

due to the inductor's role in storing energy. LC circuits, consisting of an inductor and a capacitor, demonstrate oscillatory behavior and resonance. RLC circuits, combining all three elements, showcase a rich spectrum of responses, including damped and undamped oscillations, resonance, and transient behaviors. Understanding the dynamics of these circuit models is crucial for various applications in electronics, communication systems, and signal processing, making them focal points in both theoretical analysis and practical design considerations. In recent years, there has been a growing interest in extending the analysis of electrical circuit models to the realm of fractional derivatives. This approach introduces a new dimension to the understanding of RC, RL, LC, and RLC circuit dynamics, incorporating fractional calculus principles. By considering fractional derivatives, which generalize conventional derivatives to arbitrary orders, researchers aim to capture more accurately the intricate behavior and memory effects exhibited by electrical circuits [30, 31]. In this study, we employ a sophisticated numerical approach that combines the strengths of both operational matrix and collocation methods for solving fractional-order electrical circuit models, including RL, RC, LC, and RLC configurations. Specifically, we leverage the operational matrix of fractional integration, which streamlines the complex calculations associated with fractional derivatives. This operational matrix is strategically applied to the generalized Laguerre basis vector, forming the backbone of our methodology. Subsequently, we introduce collocation by judiciously selecting equally spaced nodes, effectively transforming the fractional differential equations into a well-structured system of linear equations. This dual methodology harnesses the computational efficiency of operational matrices while benefiting from the simplicity and accuracy conferred by collocation techniques. The resulting system of linear equations is then systematically solved, providing a precise numerical solution to the intricate dynamics inherent in these electrical circuit models. This innovative combination of operational matrix and collocation methods demonstrates a powerful and versatile approach to addressing fractional order systems, showcasing its efficacy in obtaining accurate numerical solutions for a broad spectrum of electrical circuit configurations.

This paper is structured as follows: In Section 2, we lay the foundation with a discussion on fractional calculus, introducing the definitions of generalized Laguerre polynomials and their application in function approximation. Section 3 is dedicated to the construction of the generalized Laguerre operational matrix of fractional integration. Moving on to Section 4, we delve into the specific problem statements addressed in this paper and elaborate on the methodology employed, focusing on the Generalized Laguerre Operational Matrix Method (GLOMM). Section 5 is dedicated to Error Estimation based on Residual Analysis, providing a comprehensive investigation into the accuracy and reliability of our proposed approach. Section 6 presents four illustrative examples, showcasing the applicability, accuracy, and performance of our proposed technique. The paper concludes in Section 7 with a summary of findings and directions for future research.

2 Preliminaries

Definition 1 *[3] The definition of the Riemann-Liouville fractional integral of order μ for $\mathrm{Re}(\mu) > 0$ is as follows:*

$$ {}^{RL}_{a}I^{\mu}_{x} f(x) = \frac{1}{\Gamma(\mu)} \int_a^x (x-t)^{\mu-1} f(t) dt. \tag{1} $$

From the above definition, it is clear that,

$$ {}^{RL}_{0}I^{\mu}_{x}(x^p) = \frac{\Gamma(1+p)}{\Gamma(1+p+\mu)} x^{p+m}. $$

Definition 2 *[4] The definition of the Caputo fractional derivative for* $\mathrm{Re}(\mu) \geq 0$ *is as follows:*

$$ {}_a^C D_x^\mu f(x) = \frac{\mathrm{d}^n}{\mathrm{d}x^n} {}_a^{RL} I_x^{n-\mu} f(x), \qquad n := \lfloor \mathrm{Re}(\mu) \rfloor + 1. $$

The Newton–Leibniz identity establishes a fundamental relationship between the Riemann–Liouville fractional integral and the Caputo fractional derivative, expressed as follows:

$$ {}_0^{RL} I_x^\mu ({}_0^C D_x^\mu f(x)) = f(x) - \sum_{k=0}^{\lceil \mu \rceil - 1} f^{(k)}(0) \frac{x^k}{k!}. $$

Definition 3 *Consider the interval* $\Lambda = (0, \infty)$*, and let* $\omega^{(\alpha)}(x) = x^\alpha e^{-x}$ *represent a weight function in* Λ *in the conventional sense. Define*

$$ L^2_{\omega^{(\alpha)}} = \{v | v \text{ is measurable on } \Lambda \text{ and } \|v\|_{\omega^{(\alpha)}} < \infty\}, $$

with the inner product and norm

$$ (u, v)_{\omega^{(\alpha)}} = \int_\Lambda u(x) v(x) \omega^{(\alpha)}(x) dx, $$

$$ \|v\|_{\omega^{(\alpha)}} = (v, v)^{\frac{1}{2}}_{\omega^{(\alpha)}}. $$

Definition 4 *(Generalized Laguerre Polynomial) [32] Let* $L_{n,\alpha}(x)$ *be the generalized Laguerre polynomials to degree n. According to [33], for* $\alpha > -1$*, we have*

$$ L_{n+1,\alpha}(x) = \frac{1}{n+1}[(2n + \alpha - 1 - x) L_{n,\alpha}(x) - (n + \alpha) L_{n-1,\alpha}(x)], \; n = 1, 2, ..., $$

where the first few terms of the generalized Laguerre polynomials are given by

$$ \begin{aligned} L_{0,\alpha}(x) &= 1, \\ L_{1,\alpha}(x) &= 1 + \alpha - x, \\ L_{2,\alpha}(x) &= \tfrac{1}{2!}[2 + 3\alpha + \alpha^2 - 2\alpha x - 4x + x^2], \\ L_{3,\alpha}(x) &= \tfrac{1}{3!}[6 + 11\alpha + 6\alpha^2 + \alpha^3 - 13\alpha x + 3\alpha x^2 - 3\alpha^2 x - 18x + 9x^2 - x^3]. \end{aligned} $$

The analytical expression for generalized Laguerre polynomials over the interval $\Lambda = (0, \infty)$ *is given by:*

$$ L_{n,\alpha}(x) = \sum_{k=0}^{n} (-1)^k \frac{\Gamma(n + \alpha + 1)}{\Gamma(k + \alpha + 1)(n - k)! k!} x^k, \; n = 0, 1, ... \tag{2} $$

Note that, setting $\alpha = 0$ *in Eq. (2), we arrive to the classical Laguerre Polynomials* $L_n(x)$*.*

Approximation of function

A function $f(x) \in L^2_{\omega^{(\alpha)}}(\Lambda)$ can be represented using generalized Laguerre polynomials as:

$$\begin{aligned} f(x) &= \sum_{j=0}^{\infty} \psi_j L_{j,\alpha}(x), \\ \psi_j &= \frac{1}{h_r} \int_0^{\infty} f(x) L_{j,\alpha} w^{\alpha} dx, \quad j = 0, 1, 2, ... \end{aligned} \tag{3}$$

Considering the first $(N+1)$ terms of generalized Laguerre polynomials, we get

$$f \simeq f_n = \sum_{j=0}^{m} \psi_j L_{j,\alpha}(x) = \Psi^T \mathbf{L}_{m,\alpha}(x), \tag{4}$$

where the unknown coefficient vector Ψ^T and the generalized Laguerre polynomial vector $\mathbf{L}_{m,\alpha}(x)$ are defined as

$$\Psi^T = \left[\psi_0, \psi_1, \ldots, \psi_N\right]^T for\, N \in \mathrm{N}, \tag{5}$$

and

$$\mathbf{L}_{m,\alpha}(x) = \left[L_{0,\alpha}(x), L_{1,\alpha}(x), \ldots, L_{m,\alpha}(x)\right]^T for\, m \in \mathrm{N}. \tag{6}$$

3 Formulation of the generalized Laguerre operational matrix for fractional integration

In this section, we construct the operational matrix of fractional integration for the generalized Laguerre polynomials. Employing the Riemann-Liouville fractional integration (1) to the order μ on the analytical representation of generalized Laguerre polynomials $L_{i,\alpha}(x)$ provided in (2), yields:

$$\begin{aligned} I^{\mu} L_{i,\alpha}(x) &= \sum_{k=0}^{i} (-1)^k \frac{\Gamma(i+\alpha+1)}{(i-k)!k!\Gamma(k+\alpha+1)} I^{\mu} x^k \\ &= \sum_{k=0}^{i} (-1)^k \frac{\Gamma(i+\alpha+1)}{(i-k)!\Gamma(k+\alpha+1)\Gamma(k+\mu+1)} x^{k+\mu}. \end{aligned} \tag{7}$$

By approximating $x^{k+\mu}$ using $N+1$ terms of the generalized Laguerre series, we obtain:

$$x^{k+\mu} = \sum_{j=0}^{N} \psi_j L_{j,\alpha}, \tag{8}$$

where ψ_j is defined in Eq. (3) with $f(x) = x^{k+\mu}$, that is,

$$\psi_j = \sum_{r=0}^{j} (-1)^r \frac{j!\Gamma(k+\mu+\alpha+r+1)}{(j-r)!r!\Gamma(r+\alpha+1)}, \quad j = 1, 2, ..., N. \tag{9}$$

Utilizing Eqs. (7) and (8), we obtain:

$$I^{\mu}L_{i,\alpha}(x) = \sum_{j=0}^{N} D_{\mu}(i,j)L_{j,\alpha}(x), \quad i = 0,1,...,N, \tag{10}$$

where

$$D_{\mu}(i,j) := \sum_{k=0}^{i}\sum_{r=0}^{j} \frac{(-1)^{k+r} j!\Gamma(i+\alpha+1)\Gamma(k+\mu+\alpha+r+1)}{(i-k)!(j-r)!r!\Gamma(k+\mu+1)\Gamma(k+\alpha+1)\Gamma(\alpha+r+1)}. \tag{11}$$

Accordingly, Eq. (10) can be written in a vector form as follows:

$$I^{\mu}L_{i,\alpha}(x) = [D_{\mu}(i,0), D_{\mu}(i,1), ..., D_{\mu}(i,N)]\mathbf{L}_{N,\alpha}, \quad i = 0,1,...,N, \tag{12}$$

where $\mathbf{L}_{N,\alpha}$ is the generalized Laguerre vector defined in Eq. (2).
Consider $\mathbf{G}^{(\mu)}$, an operational matrix of fractional integration of order μ, with dimensions $(N+1)\times(N+1)$, defined as:

$$\mathbf{G}^{(\mu)} = \begin{pmatrix} D_{\mu}(0,0) & D_{\mu}(0,1) & D_{\mu}(0,2) & \cdots & D_{\mu}(0,N) \\ D_{\mu}(1,0) & D_{\mu}(1,1) & D_{\mu}(1,2) & \cdots & D_{\mu}(1,N) \\ \vdots & \vdots & \ddots & \vdots & \\ D_{\mu}(N,0) & D_{\mu}(N,1) & D_{\mu}(N,2) & \cdots & D_{\mu}(N,N) \end{pmatrix}.$$

Then, we can rewrite system (12) as

$$I^{\mu}\mathbf{L}_{N,\alpha}(x) = \mathbf{G}^{(\mu)}\mathbf{L}_{N,\alpha}(x). \tag{13}$$

4 Problem statement and method of solution

In this section, we delineate the specific problems at the core of our investigation and introduce the Generalized Laguerre Operational Matrix Method (GLOMM) as the key solution approach. Our focus lies on deriving numerical solutions for fractional-order electrical circuit models encompassing RL, RC, LC, and RLC configurations. By applying the GLOMM to these circuit models, we aim to provide a comprehensive and efficient numerical methodology for analyzing their fractional dynamics, contributing to the advancement of computational techniques in the field of electrical circuit modeling.

RL circuit

In this section, we focus on the numerical solutions of fractional order RL circuit. An RL circuit is an electrical circuit that consists of a resistor (R) and an inductor (L). The resistor represents the element that resists the flow of electrical current, generating heat in the process, while the inductor is a coil of wire that stores energy in its magnetic field when current flows through it. The fractional-order generalized RL circuit is given as

$$D^{\mu}u(x) + \frac{R}{L}u(x) = E(x), \quad x \in [0,1], \quad 0 < \mu \leq 1, \quad u(0) = u_0. \tag{14}$$

When $\mu = 1$, the fractional-order RL circuit equation (14) reduces to the classical case. Applying the Riemann-Liouville fractional integral of order μ to both sides of Eq. (14), we obtain:

$$u(x) - \sum_{k=0}^{\lceil \mu \rceil - 1} u^{(k)}(0)\frac{x^k}{k!} + \frac{R}{L} I^{\mu} u(x) = I^{\mu}(E(x)). \tag{15}$$

Substituting initial condition into Eq. (15) and approximating the function $u(x)$ by the generalized Laguerre polynomials (4), we get

$$\Psi^T \mathbf{L}_{m,\alpha}(x) - u_0 + \frac{R}{L}\Psi^T (I^{\mu}\mathbf{L}_{m,\alpha}(x)) = I^{\mu}(E(x)).$$

Further, using the operational matrix of fractional integration defined in Eq. (13), we obtain

$$\Psi^T \mathbf{L}_{m,\alpha}(x) + \frac{R}{L}\Psi^T (\mathbf{G}^{(\mu)}\mathbf{L}_{m,\alpha}(x)) = F(x), \tag{16}$$

where $F(x) = I^{\mu}(E(x)) + u_0$.

RC circuit

In this section, our attention shifts to the numerical analysis of the fractional order RC circuit. A RC circuit is an electrical circuit configuration comprising a resistor (R) and a capacitor (C). The resistor impedes the flow of electrical current, generating heat in the process, while the capacitor stores electrical energy in its electric field when voltage is applied across it. The fractional-order generalized RC circuit is defined as

$$D^{\mu} v(x) + \frac{1}{RC} v(x) = E(x), \quad x \in [0,1], \quad 0 < \mu \leq 1, \quad v(0) = v_0. \tag{17}$$

When $\mu = 1$, the fractional-order RC circuit equation (17) reduces to the classical case. By applying the same procedure proposed in Subsection 4 on Eq. (17), we get,

$$\Psi^T \mathbf{L}_{m,\alpha}(x) + \frac{1}{RC}\Psi^T (\mathbf{G}^{(\mu)}\mathbf{L}_{m,\alpha}(x)) = F(x), \tag{18}$$

where $F(x) = I^{\mu}(E(x)) + v_0$.

LC circuit

In this section, our focus turns to the numerical exploration of the fractional order LC circuit. The LC circuit is an electrical circuit composition consisting of an inductor (L) and a capacitor (C). The inductor stores energy in its magnetic field as current flows through it, while the capacitor stores electrical energy in its electric field when voltage is applied. The fractional-order generalized LC circuit is described as

$$LD^{\mu} q(x) + \frac{1}{C} q(x) = E(x), \quad 1 < \mu \leq 2, \quad q(0) = q_0, \quad q'(0) = q_1. \tag{19}$$

This fractional-order LC circuit equation (19) reduces to the classical one when $\mu = 2$. Applying the Riemann-Liouville fractional integral of order μ to both sides of Eq. (19) and dividing by L, we

get

$$q(x) - \sum_{k=0}^{\lceil \mu \rceil - 1} q^{(k)}(0)\frac{x^k}{k!} + \frac{1}{LC} I^{\mu} q(x) = \frac{1}{L} I^{\mu}(E(x)). \tag{20}$$

Substituting initial condition into Eq. (20) and approximating the function $q(x)$ by the generalized Laguerre polynomials (4), we get

$$\Psi^T \mathbf{L}_{m,\alpha}(x) - q_0 - xq_1 + \frac{1}{LC}\Psi^T I^{\mu} \mathbf{L}_{m,\alpha}(x) = \frac{1}{L} I^{\mu}(E(x)). \tag{21}$$

Next, using the operational matrix of fractional integration defined in Eq. (13), we obtain

$$\Psi^T \mathbf{L}_{m,\alpha}(x) + \frac{1}{LC}\Psi^T (\mathbf{G}^{(\mu)} \mathbf{L}_{m,\alpha}(x)) = F(x), \tag{22}$$

where $F(x) = \frac{1}{L} I^{\mu}(E(x)) + q_0 + xq_1$.

RLC circuit

In this section, our focus transitions to the numerical analysis of the fractional order *RLC* circuit. The *RLC* circuit is a complex electrical configuration integrating a resistor (R), an inductor (L), and a capacitor (C). The resistor hinders the flow of electrical current, the inductor stores energy in its magnetic field, and the capacitor stores electrical energy in its electric field when voltage is applied. The fractional-order generalized *RLC* circuit is characterized by

$$D^{\beta} w(x) + \frac{R}{L} D^{\mu} w(x) + \frac{1}{LC} w(x) = E(x),\ x \in [0,1], \quad 0 < \mu \leq 1, 1 < \beta \leq 2, \tag{23}$$

with

$$w^{(i)}(0) = w_i,\ i = 0, 1, ..., \lceil \beta \rceil - 1.$$

This fractional-order *RLC* circuit equation (23) reduces to the classical one when $\beta = 2$ and $\mu = 1$. Applying the R–L fractional integration to the order β on both sides of Eq. (23), we get

$$w(x) - \sum_{k=0}^{\lceil \beta \rceil - 1} w^{(k)}(0)\frac{x^k}{k!} + \frac{R}{L} I^{\beta-\mu}\left(w(x) - \sum_{k=0}^{r} w^{(k)}(0)\frac{x^k}{k!}\right) + \frac{1}{LC} I^{\beta} w(x) = I^{\beta}(E(x)), \tag{24}$$

where $r - 1 < \mu < r$.

Substituting initial condition into Eq. (24) and approximating the function $w(x)$ by the generalized Laguerre polynomials (4), we get

$$w(x) - w_0 - xw_1 + \frac{R}{L}\Psi^T I^{\beta-\mu} \mathbf{L}_{m,\alpha}(x) - \frac{R}{L} I^{\beta-\mu}\left(\sum_{k=0}^{r} w^{(k)}(0)\frac{x^k}{k!}\right) + \frac{1}{LC}\Psi^T I^{\beta} \mathbf{L}_{m,\alpha}(x) = I^{\beta}(E(x)). \tag{25}$$

Next, using the operational matrix of fractional integration defined in Eq. (13), we obtain

$$w(x) + \frac{R}{L}\Psi^T(\mathbf{G}^{(\beta-\mu)}\mathbf{L}_{m,\alpha}(x)) + \frac{1}{LC}\Psi^T(\mathbf{G}^{(\beta)}\mathbf{L}_{m,\alpha}(x)) = F(x), \tag{26}$$

where $F(x) = I^{\beta}(E(x)) + w_0 + xw_1 + \frac{R}{L}I^{\beta-\mu}\left(\sum_{k=0}^{r} w^{(k)}(0)\frac{x^k}{k!}\right)$.

Finally, by using the collacation points $x_i = \frac{i}{N}$ where $i = 0, 1, \cdots, N$ in Eqs. (16), (18), (22) and (26), we get a system of $N+1$ algebraic equations for each circuit model [34]. Solving these systems of algebraic equations for the unknown vector Ψ^T and using Eq. (4), we get an accurate approximation solution to the given models.

5 Error analysis

In this section, we introduce an error estimation method based on the residual error function for our proposed GLOMM. The residual error, a quantification of the difference between computed and true solutions in numerical methods, serves as a pivotal tool in assessing accuracy and convergence. By monitoring the residual during the solution process, it offers insights into method convergence, facilitates error control, and aids in adaptive strategies.

Consider the general fractional-order electrical circuit equation:

$$D^{\beta}y(x) + AD^{\mu}y(x) + By(x) = E(x),\ x \in [0,1], \quad 0 < \mu \leq 1, \quad 1 < \beta \leq 2, \tag{27}$$

with

$$y^{(i)}(0) = y_i,\ i = 0, 1, ..., \lceil\beta\rceil - 1,$$

where D^{β} and D^{μ} represent the fractional derivative of order β and μ, respectively. A and B are coefficients related to the circuit components (e.g. resistance, inductance, capacitance). Let $y_N(x)$ be the numerical solution of given initial value problem (27). Substituting $y_N(x)$ into Eq. (27), we get

$$D^{\beta}y_N(x) + AD^{\mu}y_N(x) + By_N(x) - E(x) = R_N(x), \tag{28}$$

where $R_N(x)$ is the residual function. By using Eqs. (27) and (28), we get

$$D^{\beta}(y(x) - y_N(x)) + AD^{\mu}(y(x) - y_N(x)) + B(y(x) - y_N(x)) = R_N(x). \tag{29}$$

Now, let us define the error function as $\epsilon_N(x) = (y(x) - y_N(x))$. Subsequently, employing this error function in Eq. (29), we derive

$$D^{\beta}\epsilon_N(x) + AD^{\mu}\epsilon_N(x) + B\epsilon_N(x) = R_N(x), \tag{30}$$

with initial conditions $\epsilon_N(0) = 0$ and $\epsilon'_N(0) = 0$. Solving Eq. (30) using the approach outlined in Section 4 yields the approximate error estimation $\epsilon_N(x)$ for the proposed method. Consequently, the approximation of maximum absolute error can be estimated by

$$E_N = \max|\epsilon_N|, \quad 0 \leq x \leq T.$$

6 Numerical simulations and comparative discussions

In this section, we illustrate the dynamics of fractional electrical circuit models, specifically RL, RC, LC, and RLC, through four distinct examples. These demonstrations showcase the efficacy of the Generalized Laguerre Operational Matrix Method (GLOMM) under various fractional derivative orders. To validate the accuracy and versatility of our proposed method, we conduct comprehensive comparisons with existing techniques reported in the literature. This comparative analysis serves as a robust means of affirming the reliability and applicability of the GLOMM in accurately capturing the behavior of fractional electrical circuit models across different fractional derivative orders. All computations are performed using Matlab R2021a.

Example 1 *(RL Circuit) In this illustrative instance, we contemplate the fractional-order RL circuit model defined by Eq. (14) in the presence of a constant voltage source, where $E(x) = 0$. Specifically, when considering $\mu = 1$, the precise solution to Eq. (14) can be expressed as*

$$u(x) = \left[u_0 - \frac{E(x)L}{R}\right] e^{\frac{-R}{L}x} + \frac{E(x)L}{R}.$$

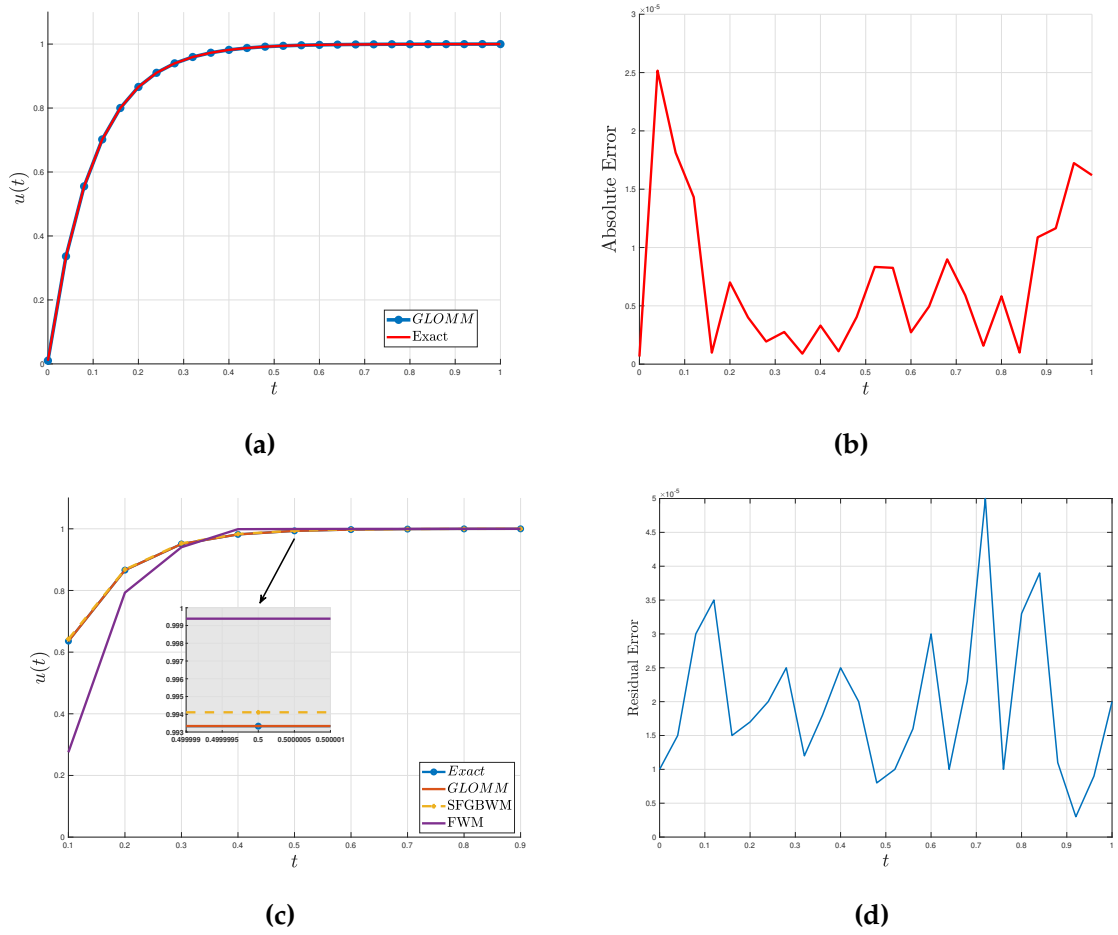

Figure 1. (a) Comparative illustration of approximate solutions for the fractional-order RL circuit in contrast to the exact solution. (b) Absolute error obtained from GLOMM. (c) Comparative illustration of exact, GLOMM, SFGBWM, and FWM solutions for the RL circuit model at $\mu = 1.00$. (d) Residual error estimation for RL circuit model

In Figure 1a, we present a visual comparison between the exact solution and the approximation obtained through the Generalized Laguerre Operational Matrix Method (GLOMM), as introduced in Subsection 4, for the fractional-order RL circuit. The analysis involves specific parameter values $R = 10$, $L = 1$, an initial condition of $u_0 = 10$, and a derivative order of $\mu = 1$. Additionally, Figure 1b illustrates the associated absolute error resulting from the application of GLOMM to the RL circuit under the same settings. In Figure 1c, a graphical comparison unfolds between the exact solution, our proposed method, and established methods from the literature, namely Shifted fractional order Gegenbauer wavelets method (SFGBWM) [25] and Fibonacci wavelet (FWM) [26]. The visual representation distinctly highlights the remarkable alignment between our method and the exact solution, showcasing its superior performance compared to existing approaches. Figure 1d illustrates the estimation results of the residual error function for the RL circuit model. These estimation results demonstrate a concordance between the absolute error and the estimated error, both of which are around 10^{-5}, showcasing the accuracy of the proposed method.

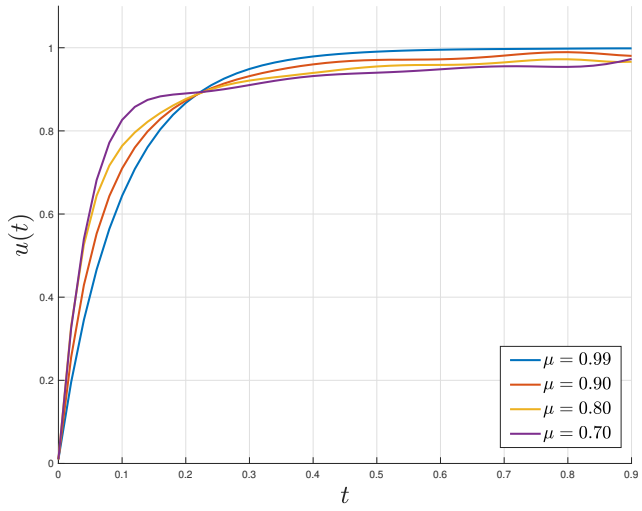

(a)

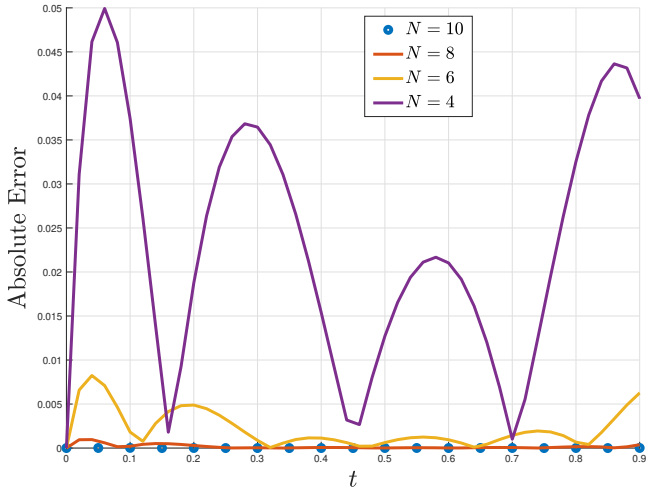

(b)

Figure 2. (a) Dynamic response of GLOMM solution for the *RL* circuit at varying values of the fractional parameter μ. (b) Absolute errors for the *RL* circuit at different N values

In Figure 2a, we depict the graphical behavior of the RL circuit across various fractional derivative orders, specifically for $\mu = 0.99, 0.90, 0.80, 0.70$. This illustration unveils the dynamic response of the RL circuit model to alterations in fractional derivative orders. Notably, as the fractional derivative order diminishes, the function reaches its maximum value at an earlier stage. This trend indicates that a lower fractional derivative order induces an expedited response in the RL circuit, leading to a more rapid attainment of its peak value. In Figure 2b, we showcase the absolute errors derived from the application of GLOMM with varying numbers of basis vectors for generalized Laguerre polynomials, specifically for $N = 4, 6, 8, 10$. This graphical representation highlights an improved performance of GLOMM with increasing values of N, indicating enhanced accuracy and convergence as the number of basis vectors for Laguerre polynomials expands.

Example 2 *(RC Circuit) In this illustration, we examine the fractional-order RC circuit model as defined by Eq. (17), assuming a constant voltage source with $E(x) = 0$. When $\mu = 1$, the precise solution to Eq. (17) is obtained as*

$$v(x) = v_0 e^{\frac{-x}{RC}}.$$

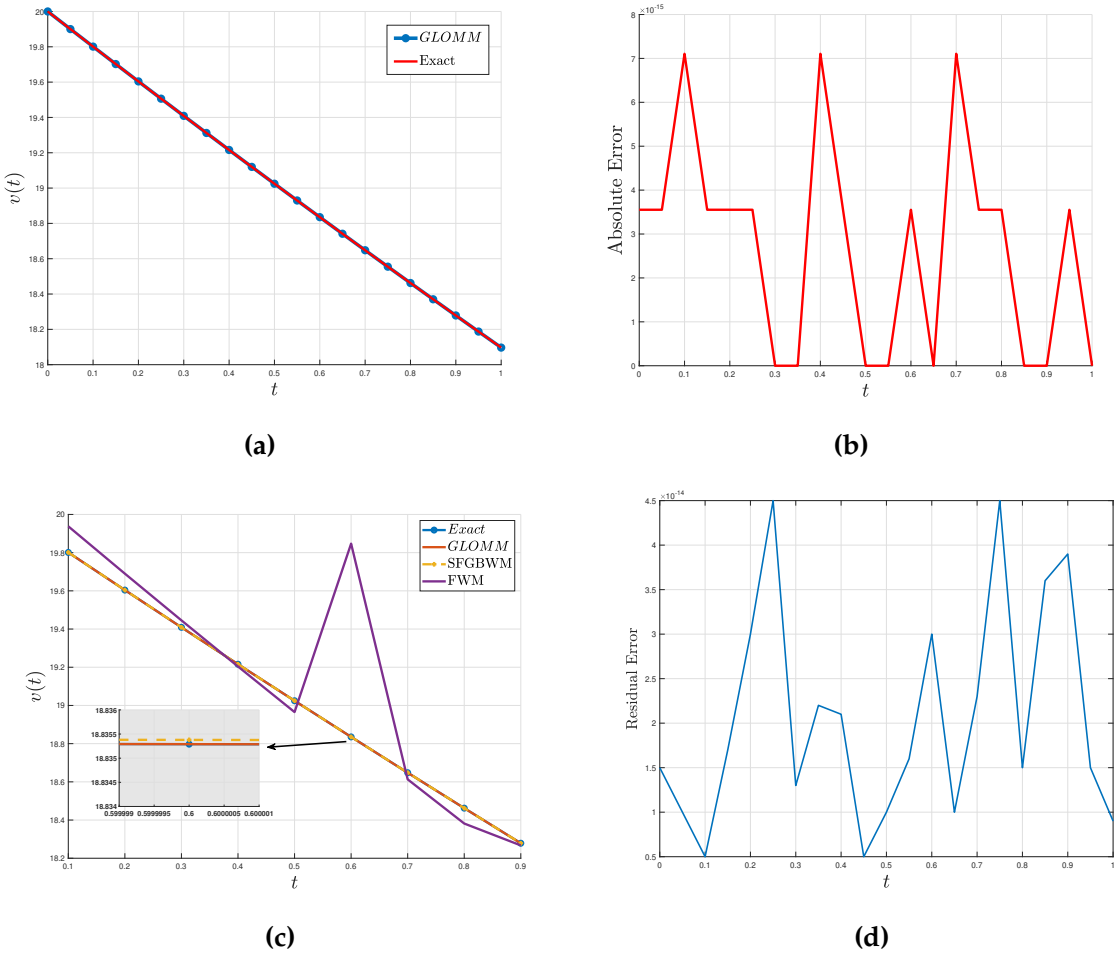

Figure 3. (a) Comparative illustration of approximate solutions for the fractional-order RC circuit in contrast to the exact solution. (b) Absolute error obtained from GLOMM. (c) Comparative illustration of exact, GLOMM, SFGBWM, and FWM solutions for the RC circuit model at $\mu = 1.00$. (d) Residual error estimation for RC circuit model

In Figure 3a, we present a visual juxtaposition of the exact solution and the approximation achieved through the GLOMM, as introduced in Subsection 4, for the fractional-order RC circuit. The analysis encompasses specific parameter values $R = 10$, $C = 1$, an initial condition of $v_0 = 20$, and a derivative order of $\mu = 1$. Furthermore, Figure 3b illustrates the corresponding absolute error resulting from the application of GLOMM to the RC circuit under the same settings. In Figure 3c, a graphical comparison unfolds between the exact solution, our proposed method, and established methods from the literature, namely the SFGBWM [25] and FWM [26]. The visual representation distinctly highlights the notable alignment between our method and the exact solution, underscoring its superior performance relative to existing approaches. Figure 3d illustrates the estimation results of the residual error function for the RC circuit model. These estimation results demonstrate an agreement between the absolute error and the estimated error.

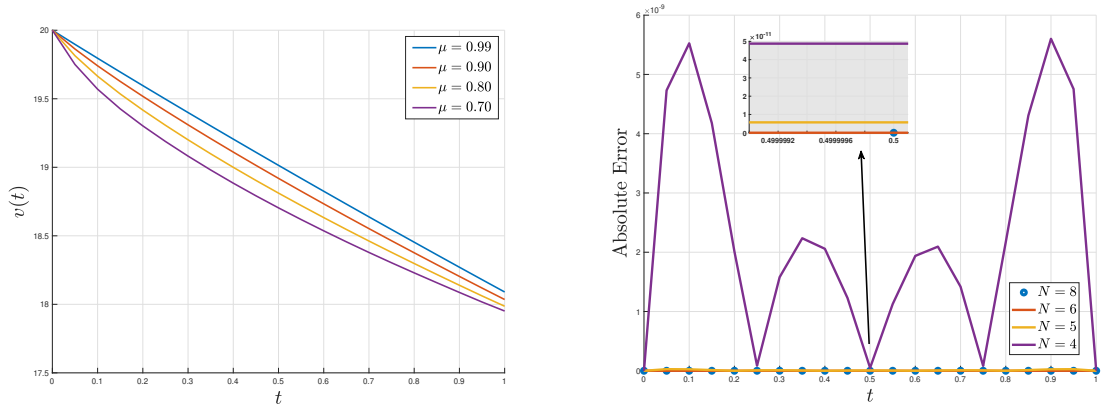

(a) **(b)**

Figure 4. (a) Dynamic response of GLOMM solution for the *RC* circuit at varying values of the fractional parameter μ. (b) Absolute errors for the *RC* circuit at different N values

In Figure 4a, we depict the graphical behavior of the fractional-order RC circuit across various fractional derivative orders, specifically for $\mu = 0.99, 0.90, 0.80, 0.70$. In Figure 4b, we present the absolute errors resulting from the application of GLOMM with different numbers of basis vectors for generalized Laguerre polynomials, specifically considering $N = 4, 5, 6, 8$. This graphical representation underscores the improved performance of GLOMM as the value of m increases, suggesting enhanced accuracy and convergence with the expansion of the number of basis vectors for generalized Laguerre polynomials. In the subsequent analysis, we alter the configuration for the fractional-order RC circuit by setting $R = 1$ and applying GLOMM under a fractional order of $\mu = 0.5$.

Table 1 provides a comparative analysis of solutions obtained using the GLOMM, ABM, and Ch3WM for the fractional-order RC circuit model. The analysis is conducted under a fractional derivative order of $\mu = 0.5$. The resulting outcomes are visually compared with established techniques, such as the Chebyshev Wavelets of the third kind Method (Ch3WM) [24], in Figure 5. Given that the exact solution of the RC circuit is defined for integer derivative orders, rendering it unsuitable as a reference under fractional order $\mu = 0.5$, we employ the Adams-Bashforth method (ABM) [35] as a reference technique. The comparison between our method, Ch3WM, and ABM reveals a notable alignment. The obtained results strongly indicate that GLOMM exhibits superior agreement compared to other techniques.

Table 1. Comparison of GLOMM, Ch3WM, and ABM solutions for fractional order RC circuit model with $\mu = 0.5$

	ABM	GLOMM	Ch3WM
0	0.01	0.010006099	0.009311492
0.1	0.007280578	0.007195621	0.007227947
0.2	0.006459239	0.006429888	0.006437929
0.3	0.005940309	0.005921566	0.005920666
0.4	0.005555113	0.005525782	0.005536186
0.5	0.005249442	0.005209207	0.005231222
0.6	0.004996976	0.004985988	0.004980178
0.7	0.004782689	0.004785824	0.004766949
0.8	0.004597144	0.004561122	0.00458242
0.9	0.004434009	0.004411648	0.004420164

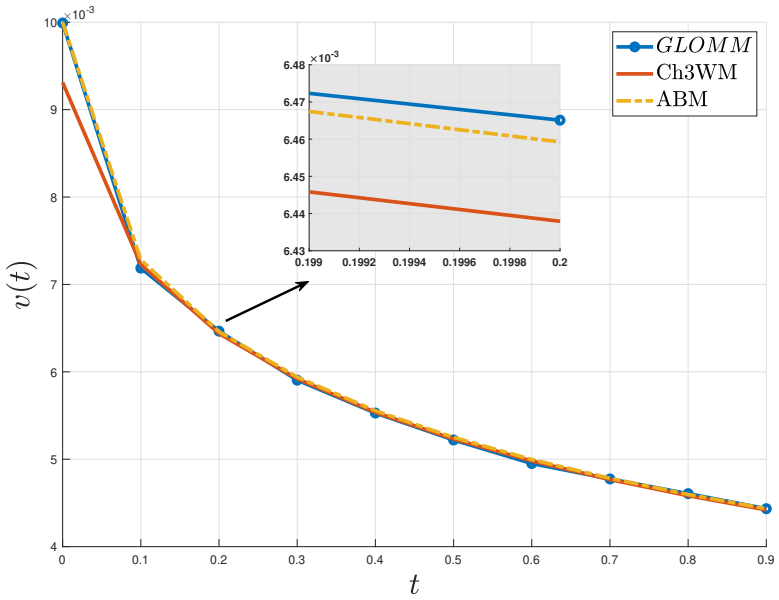

Figure 5. Comparative illustration of GLOMM, Ch3WM, and ABM solutions for the RC circuit model at $\mu = 0.5$

Example 3 *(LC Circuit) In this instance, we examine the fractional-order LC circuit model described by Eq. (19). Assuming a constant voltage source with $E(x) = 0$, the precise solution to Eq. (19) is derived for $\mu = 2$ as follows:*

$$q(x) = q_0 cos\left(\sqrt{\frac{1}{LC}}x\right) + CE(x) - CE(x)cos\left(\sqrt{\frac{1}{LC}}x\right).$$

In Figure 6a, we showcase a visual comparison between the exact solution and the approximation obtained through GLOMM, as introduced in Subsection 4, for the fractional-order LC circuit. The analysis considers specific parameter values $L = 10$, $C = 1$, an initial condition of $q_0 = 0.01$, and a derivative order of $\mu = 2$. Additionally, Figure 6b illustrates the corresponding absolute error resulting from the application of GLOMM to the LC circuit under the same settings. In Figure 6c, a graphical comparison unfolds between the exact solution, our proposed method, and established methods from the literature, namely SFGBWM [25] and FWM [26]. The visual representation distinctly highlights the remarkable alignment between our method and the exact solution, emphasizing its superior performance compared to existing

approaches. Moreover, in Figure 6d, we depict the comparison between GLOMM and the exact solution of the fractional-order LC circuit model over an extended time interval, $t \in [0, 10]$. This illustration underscores the high accuracy demonstrated by GLOMM, particularly for longer time intervals. Figure 6e illustrates the estimation results of the residual error function for the LC circuit model. These estimation results demonstrate an agreement between the absolute error and the estimated error, both of which are around 10^{-15}.

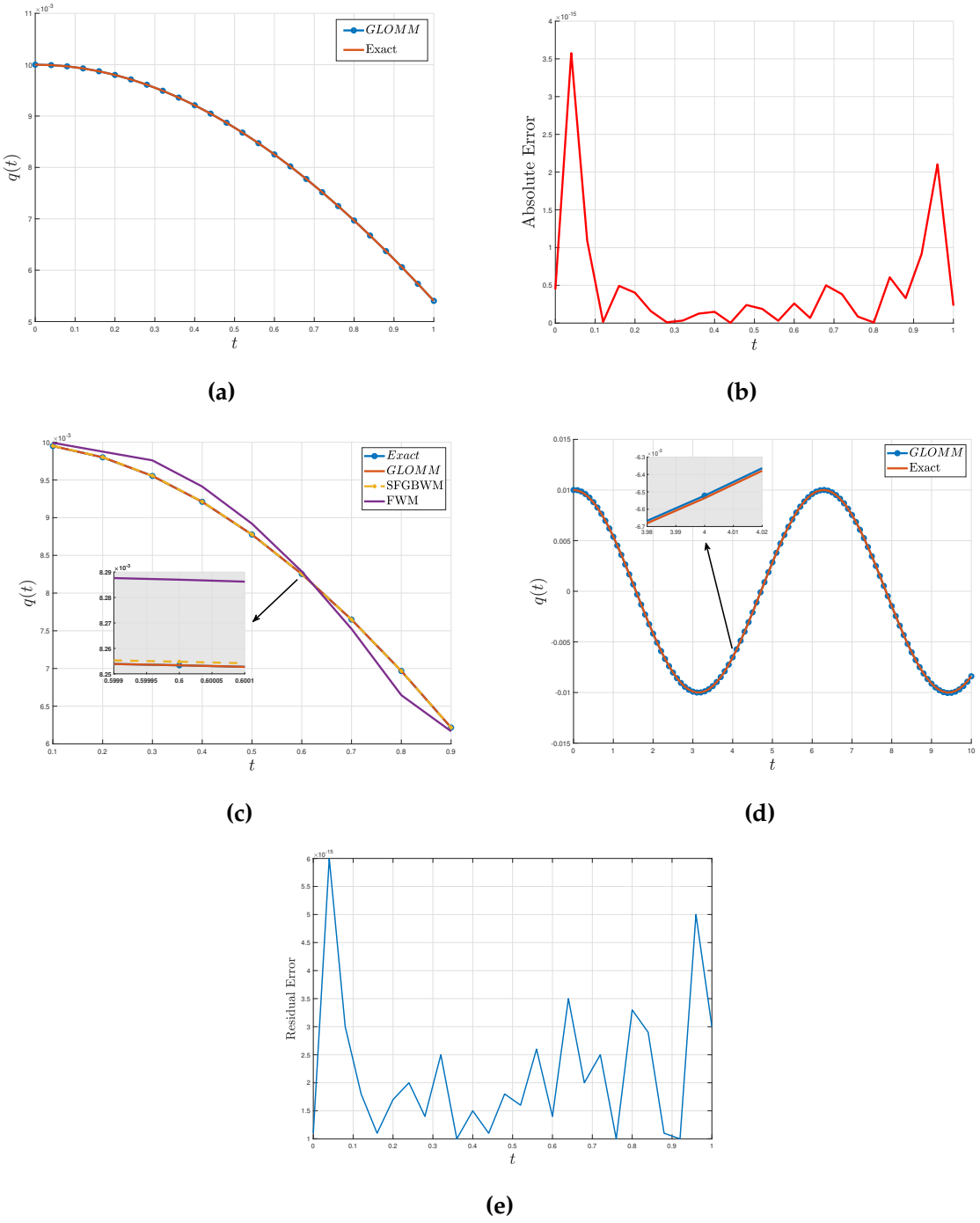

Figure 6. (a) Comparative illustration of approximate solutions for the fractional-order *LC* circuit in contrast to the exact solution. (b) Absolute error obtained from GLOMM. (c) Comparative illustration of exact, GLOMM, SFGBWM, and FWM solutions for the *LC* circuit model at $\mu = 2.00$. (d) Comparison of fractional-order *LC* circuit solutions with the exact solution for $t \in [0, 10]$. (e) Residual error estimation for *LC* circuit model

In Figure 7a, we illustrate the graphical behavior of the fractional-order LC circuit across varying fractional derivative orders, specifically for $\mu = 1.99, 1.90, 1.80, 1.70$. Concurrently, in Figure 7b, we present the absolute errors resulting from the application of GLOMM with varying numbers of basis vectors for generalized Laguerre polynomials, specifically considering $N = 5, 6, 7, 8$. This graphical representation underscores the improved performance of GLOMM as the value of m increases, indicating enhanced accuracy and convergence with the expansion of the number of basis vectors for Laguerre polynomials.

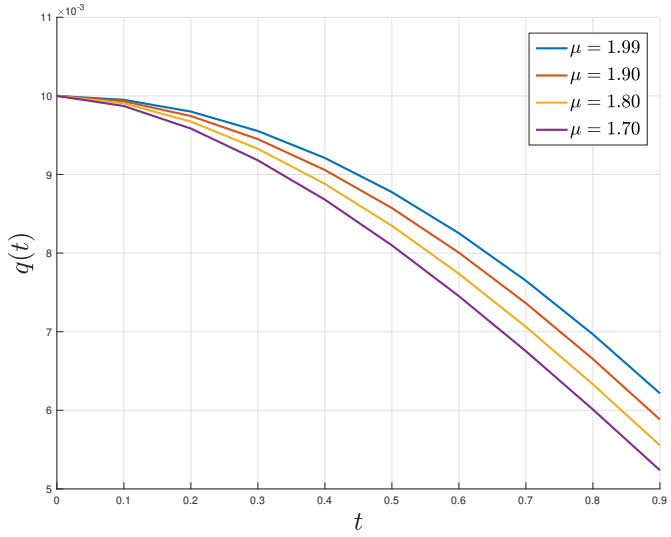

(a)

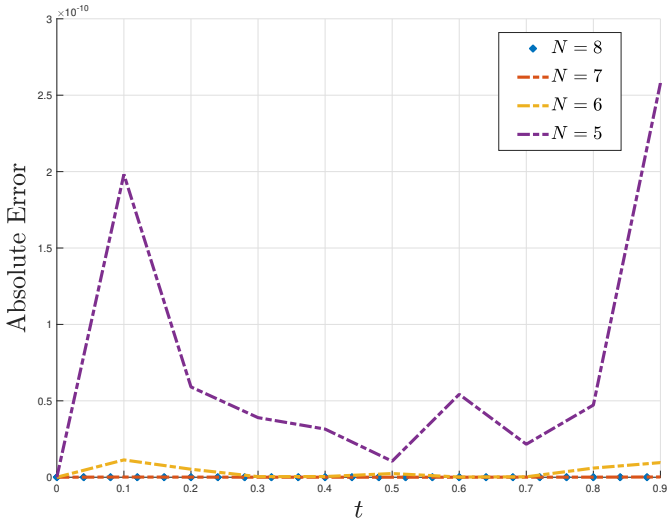

(b)

Figure 7. (a) Dynamic response of GLOMM solution for the *LC* circuit at varying values of the fractional parameter μ. (b) Absolute errors for the *LC* circuit at different N values

In Figure 8, we modify the configuration for the fractional-order LC circuit by setting $\mu = 1.5$ and applying GLOMM. The resulting outcomes are visually contrasted with well-established techniques, such as the Bernoulli Wavelet Method (BWM) [24]. Considering that the exact solution of the LC circuit is defined for integer derivative orders, making it unsuitable as a reference under fractional order $\mu = 1.5$, we again resort to the ABM [35] as a reference technique. The comparison involving our method, BWM, and ABM

reveals a noteworthy alignment. The obtained results strongly indicate that GLOMM exhibits superior agreement compared to other techniques.

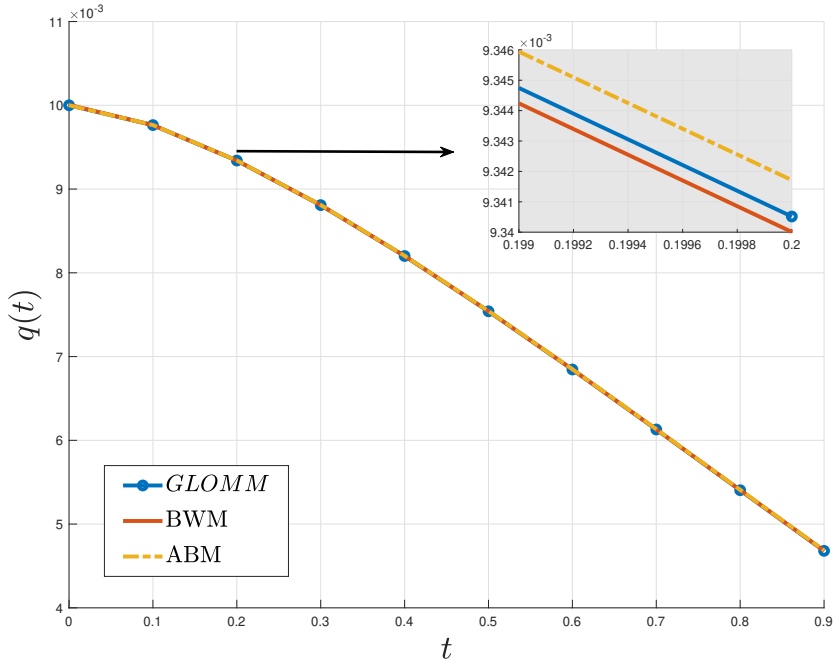

Figure 8. Comparative illustration of GLOMM, BWM, and ABM solutions for the *LC* circuit model at $\mu = 1.5$

Table 2 provides a comparative analysis of solutions obtained using the GLOMM, ABM, and BWM for the fractional-order LC circuit model. The analysis is conducted under a fractional derivative order of $\mu = 1.7$.

Table 2. Comparison of GLOMM, BWM, and ABM solutions for fractional order *LC* circuit model with $\mu = 1.7$

	ABM	GLOMM	BWM
0	0.01	0.01	0.010001716
0.1	0.009871448	0.009871159	0.009870358
0.2	0.009585093	0.009584501	0.009583816
0.3	0.009181335	0.009180212	0.009179646
0.4	0.008681298	0.008679638	0.008679286
0.5	0.008101184	0.008098930	0.008099095
0.6	0.007454966	0.007452128	0.007452203
0.7	0.006755332	0.006751900	0.006752166
0.8	0.006014079	0.006010103	0.006010442
0.9	0.005242306	0.005237790	0.00523831

Example 4 *(RLC Circuit) In this instance, we delve into the RLC circuit model described by Eq. (23). Assuming a constant voltage source with* $E(x) = 0$, *the exact solution to Eq. (23) is derived for* $\beta = 2$ *and* $\mu = 1$ *as follows:*

$$w(x) = w_0 e^{\frac{-Rx}{2L}} cos\left(\sqrt{\frac{1}{LC} - \frac{R^2}{4L^2}}x\right).$$

In Figure 9a, we present a visual comparison between the exact solution and the approximation obtained through GLOMM, as introduced in Subsection 4, for the fractional-order RLC circuit. The analysis considers specific parameter values $R = 10$, $L = 10$, $C = 10$, *an initial condition of* $w_0 = 0.01$, *and derivative orders* $\beta = 2$ *and* $\mu = 1$. *Additionally, in Figure 9b, we illustrate the graphical behavior of the fractional-order RLC circuit across varying fractional derivative orders, specifically for* $\beta = 2.00, \mu = 1.00$, $\beta = 1.90, \mu = 0.95$, $\beta = 1.80, \mu = 0.90$, $\beta = 1.70, \mu = 0.85$, $\beta = 1.60, \mu = 0.80$, *and* $\beta = 1.50, \mu = 0.75$.

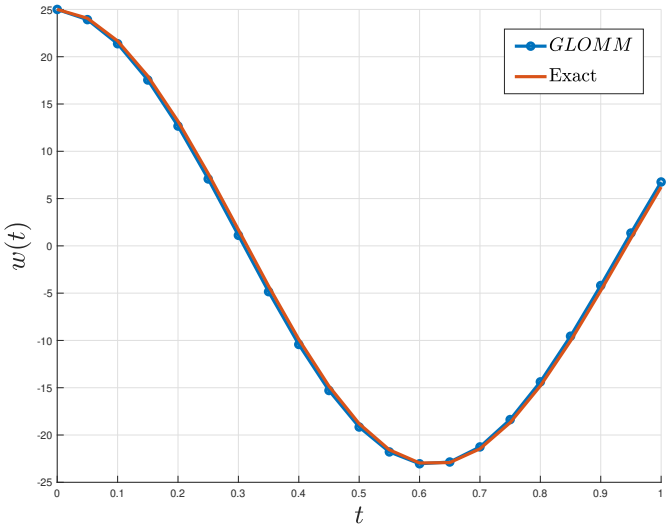

(a)

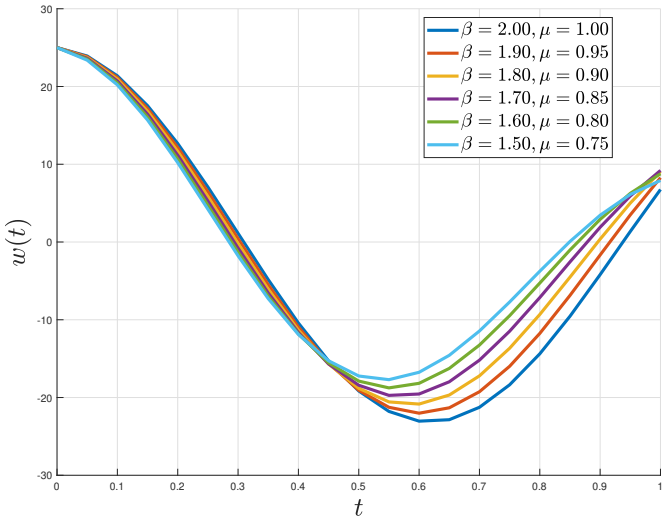

(b)

Figure 9. (a) Comparative illustration of approximate solutions for the fractional-order *RLC* circuit in contrast to the exact solution. (b) Dynamic response of GLOMM solution for the *RLC* circuit at varying values of the fractional parameters β and μ

Table 3 showcases the CPU time (in seconds) required for solving RC, RL, LC, and RLC circuits utilizing the Generalized Laguerre Operational Matrix Method. These results underscore the ability of GLOMM to deliver fast and efficient numerical solutions, making it a promising technique for applications that demand

both accuracy and computational speed.

Table 3. CPU time (in seconds)

	RC	*RL*	*LC*	*RLC*
CPU time(s)	0.3081	0.3025	0.2812	0.3438

In Table 4, we provide a comprehensive comparison of the maximum absolute errors achieved by our proposed GLOMM in contrast to FWM, SFGWM, and BWM for the RC, RL, and LC electrical circuit models. This comparison emphasizes the superior accuracy and precision of GLOMM in delivering numerical solutions for fractional-order electrical circuits.

Table 4. Comparison of Maximum Absolute Errors for *RC*, *RL*, and *LC* circuits

	GLOMM	FWM	SFGWM	BWM
RC	7.1054×10^{-15}	9.7149×10^{-5}	9.6041×10^{-5}	6.11×10^{-2}
RL	2.1278×10^{-5}	5.5706×10^{-4}	6.7269×10^{-3}	-
LC	3.2682×10^{-15}	1.6238×10^{-6}	2.8394×10^{-6}	1.16×10^{-5}

7 Conclusion and further research

In conclusion, this research introduces a novel and efficient numerical approach, the Generalized Laguerre Operational Matrix Method (GLOMM), for solving fractional electrical circuit models represented by *RL*, *RC*, *LC*, and *RLC* configurations within the framework of the Caputo derivative. By leveraging the distinctive properties of generalized Laguerre polynomials and developing an operational matrix of fractional integration, our method offers a powerful tool for accurately capturing the intricate dynamics of these circuits. Through a series of numerical examples conducted using Matlab R2021a, we demonstrated the robustness and versatility of our proposed approach across varying fractional derivative orders. Notably, we observed maximum absolute errors of approximately 10^{-15} for the *RC* circuit, 10^{-5} for the *RL* circuit, and 10^{-15} for the *LC* circuit, highlighting the superior accuracy of our method compared to existing approaches. Furthermore, the high level of agreement in the approximate solution for the *RLC* circuit, as evidenced in the illustrations, further validates the efficacy of our approach. Additionally, CPU time serves as a crucial metric for assessing computational efficiency, directly reflecting the computational resources required to execute our algorithm. The maximum CPU time of 0.3438 obtained using GLOMM underscores the computational efficiency of our proposed technique. The results underscore the potential of our method as a valuable tool in the analysis and design of fractional electrical circuits, showcasing its ability to provide precise solutions and enhance our understanding of the underlying dynamic behaviors.

Future research directions stemming from this study could explore the extension of the GLOMM to address nonlinear fractional electrical circuit models, assessing its performance under varying degrees of nonlinearity. Additionally, incorporating alternative orthogonal basis functions or operational matrices alongside generalized Laguerre polynomials may be investigated to enhance the method's versatility. Parametric studies and sensitivity analyses can be conducted to evaluate the robustness of the GLOMM in response to variations in circuit parameters and fractional orders. In addition, integration with machine learning techniques could be explored to optimize the selection of collocation nodes and further refine the approximation process, ultimately improving the accuracy and efficiency of the GLOMM.

Declarations

Use of AI tools

The author declares that he has not used Artificial Intelligence (AI) tools in the creation of this article.

Data availability statement

All data generated or analyzed during this study are included in this article.

Ethical approval

The author states that this research complies with ethical standards. This research does not involve either human participants or animals.

Consent for publication

Not applicable

Conflicts of interest

The author declares that he has no conflict of interest.

Funding

Not applicable

Author's contributions

The author has read and agreed to the published version of the manuscript.

Acknowledgements

Not applicable

References

[1] Machado, J.T., Kiryakova, V. and Mainardi, F. Recent history of fractional calculus. *Communications in Nonlinear Science and Numerical Simulation*, 16(3), 1140-1153, (2011). [CrossRef]

[2] Miller, K.S. and Rosso, B. *An Introduction to the Fractional Calculus and Fractional Differential Equations*. Wiley: New York, (1993).

[3] Oldhalm, K.B. and Spainer, J. *The Fractional Calculus*. Academic Press: New York, USA, (1974).

[4] Caputo, M. Linear models of dissipation whose Q is almost frequency independent—II. *Geophysical Journal International*, 13(5), 529-539, (1967). [CrossRef]

[5] Debnath, L. Recent applications of fractional calculus to science and engineering. *International Journal of Mathematics and Mathematical Sciences*, 2003, 3413-3442, (2003). [CrossRef]

[6] Tarasov, V.E. Mathematical economics: application of fractional calculus. *Mathematics*, 8(5), 660, (2020). [CrossRef]

[7] Alinei-Poiana, T., Dulf, E.H. and Kovacs, L. Fractional calculus in mathematical oncology. *Scientific Reports*, 13, 10083, (2023). [CrossRef]

[8] Mainardi, F. *Fractional Calculus and Waves in Linear Viscoelasticity: An Introduction to Mathematical Models*. World Scientific: Singapore, (2022). [CrossRef]

[9] Avcı, İ., Lort, H. and Tatlıcıoğlu, B.E. Numerical investigation and deep learning approach for fractal–fractional order dynamics of Hopfield neural network model. *Chaos, Solitons & Fractals*, 177, 114302, (2023). [CrossRef]

[10] Chen, S.B., Soradi-Zeid, S., Jahanshahi, H., Alcaraz, R., Gómez-Aguilar, J.F., Bekiros, S. et al. Optimal control of time-delay fractional equations via a joint application of radial basis functions and collocation method. *Entropy*, 22(11), 1213, (2020). [CrossRef]

[11] Joshi, H. and Yavuz, M. Transition dynamics between a novel coinfection model of fractional-order for COVID-19 and tuberculosis via a treatment mechanism. *The European Physical Journal Plus*, 138, 468, (2023). [CrossRef]

[12] Soradi-Zeid, S., Jahanshahi, H., Yousefpour, A. and Bekiros, S. King algorithm: a novel optimization approach based on variable-order fractional calculus with application in chaotic financial systems. *Chaos, Solitons & Fractals*, 132, 109569, (2020). [CrossRef]

[13] Rezapour, S., Asamoah, J.K.K., Etemad, S., Akgül, A., Avcı, İ. and El Din, S.M. On the fractal-fractional Mittag-Leffler model of a COVID-19 and Zika Co-infection. *Results in Physics*, 55, 107118, (2023). [CrossRef]

[14] Zhao, W., Leng, K., Chen, J., Jiao, Y. and Zhao, Q. Research on statistical algorithm optimization of fractional differential equations of quantum mechanics in ecological compensation. *The European Physical Journal Plus*, 134, 316, (2019). [CrossRef]

[15] Duran, S., Durur, H., Yavuz, M. and Yokus, A. Discussion of numerical and analytical techniques for the emerging fractional order murnaghan model in materials science. *Optical and Quantum Electronics*, 55, 571, (2023). [CrossRef]

[16] Yilmaz, B. A new type electromagnetic curves in optical fiber and rotation of the polarization plane using fractional calculus. *Optik*, 247, 168026, (2021). [CrossRef]

[17] Barros, L.C.D., Lopes, M.M., Pedro, F.S., Esmi, E., Santos, J.P.C.D. Sánchez, D.E. et al. The memory effect on fractional calculus: an application in the spread of COVID-19. *Computational and Applied Mathematics*, 40, 72, (2021). [CrossRef]

[18] Tarasov, V.E. On history of mathematical economics: application of fractional calculus. *Mathematics*, 7(6), 509, (2019). [CrossRef]

[19] El-Gamel, M., Mohamed, N. and Waleed, A. Genocchi collocation method for accurate solution of nonlinear fractional differential equations with error analysis. *Mathematical Modelling and Numerical Simulation with Applications*, 3(4), 351-375, (2023). [CrossRef]

[20] Wu, G.C. A fractional variational iteration method for solving fractional nonlinear differential equations. *Computers & Mathematics with Applications*, 61(8), 2186-2190, (2011). [CrossRef]

[21] Mohamed, S.A. A fractional differential quadrature method for fractional differential equations and fractional eigenvalue problems. *Mathematical Methods in the Applied Sciences*, (2020). [CrossRef]

[22] Albogami, D., Maturi, D. and Alshehri, H. Adomian decomposition method for solving fractional Time-Klein-Gordon equations using Maple. *Applied Mathematics*, 14(6), 411-418, (2023). [CrossRef]

[23] Abuasad, S., Hashim, I. and Abdul Karim, S.A. Modified fractional reduced differential transform method for the solution of multiterm time-fractional diffusion equations. *Advances in Mathematical Physics*, 2019, 5703916, (2019). [CrossRef]

[24] Tural-Polat, S.N. and Dincel, A.T. Wavelet methods for fractional electrical circuit equations.

Physica Scripta, 98(11), 115203, (2023). [CrossRef]

[25] Yadav, P., Jahan, S. and Nisar, K.S. Shifted fractional order Gegenbauer wavelets method for solving electrical circuits model of fractional order. *Ain Shams Engineering Journal*, 14(11), 102544, (2023). [CrossRef]

[26] Ahmed, S., Shah, K., Jahan, S. and Abdeljawad, T. An efficient method for the fractional electric circuits based on Fibonacci wavelet. *Results in Physics*, 52, 106753, (2023). [CrossRef]

[27] Li, M., Huang, C. and Wang, P. Galerkin finite element method for nonlinear fractional Schrödinger equations. *Numerical Algorithms*, 74, 499-525, (2017). [CrossRef]

[28] Zafarghandi, F.S., Mohammadi, M., Babolian, E. and Javadi, S. Radial basis functions method for solving the fractional diffusion equations. *Applied Mathematics and Computation*, 342, 224-246, (2019). [CrossRef]

[29] Alexander, C.K. *Fundamentals of Electric Circuits*. McGraw-Hill, (2013).

[30] Kaczorek, T. and Rogowski, K. Positive fractional electrical circuits. In *Fractional Linear Systems and Electrical Circuits* (Vol. 13) (pp. 49-80). Switzerland: Springer Cham, (2015). [CrossRef]

[31] Ibrahim Nuruddeen, R., Gómez-Aguilar, J.F., Garba Ahmad, A. and Ali, K.K. Investigating the dynamics of Hilfer fractional operator associated with certain electric circuit models. *International Journal of Circuit Theory and Applications*, 50(7), 2320-2341, (2022). [CrossRef]

[32] Bhrawy, A.H., Baleanu, D., Assas, L.M. and Tenreiro Machado, J.A. On a generalized Laguerre operational matrix of fractional integration. *Mathematical Problems in Engineering*, 2013, 569286, (2013). [CrossRef]

[33] Dimitrov, D.K., Marcellán, F. and Rafaeli, F.R. Monotonicity of zeros of Laguerre–Sobolev-type orthogonal polynomials. *Journal of Mathematical Analysis and Applications*, 368(1), 80-89, (2010). [CrossRef]

[34] Avcı, İ. Numerical simulation of fractional delay differential equations using the operational matrix of fractional integration for fractional-order Taylor basis. *Fractal and Fractional*, 6(1), 10, (2021). [CrossRef]

[35] Diethelm, K., Ford, N.J. and Freed, A.D. Detailed error analysis for a fractional Adams method. *Numerical Algorithms*, 36, 31-52, (2004). [CrossRef]

Mathematical Modelling and Numerical Simulation with Applications (MMNSA)
(https://dergipark.org.tr/en/pub/mmnsa)

How to cite this article: Avcı, İ. (2024). Spectral collocation with generalized Laguerre operational matrix for numerical solutions of fractional electrical circuit models. *Mathematical Modelling and Numerical Simulation with Applications*, 4(1), 110-132. https://doi.org/10.53391/mmnsa.1428035